

Increasing Hydrophobicity of Nanoparticles Intensifies Lung Surfactant Film Inhibition and Particle Retention

Russell P. Valle,[†] Charlotte Liwen Huang,[‡] Joachim S. C. Loo,^{‡,§} and Yi Y. Zuo^{*,†}

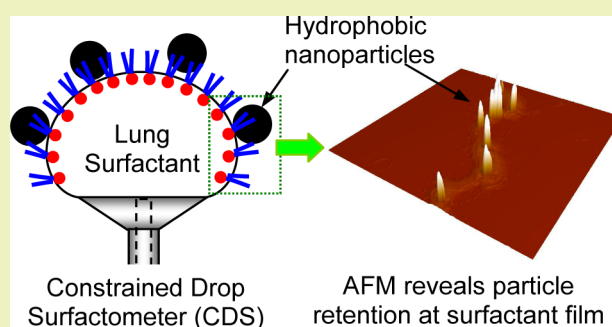
[†]Department of Mechanical Engineering, University of Hawaii at Manoa, Honolulu, Hawaii 96822, United States

[‡]School of Materials Science & Engineering, Nanyang Technological University, Singapore 639798

[§]Singapore Centre on Environmental Life Sciences Engineering, Nanyang Technological University, Singapore 637551

ABSTRACT: Polymeric nanoparticles (NPs) have had much focus on their ability to penetrate deep pulmonary structures as potential drug carriers. However, research on the toxicological effects of NPs is in its infancy, and interaction mechanisms are largely unknown. Studies have shown that the interactions with pulmonary structures are heavily dependent on the physicochemical properties of the NPs. Here, we studied how hydrophobicity of polymeric NPs affect pulmonary surfactant biophysics *in vitro*. We investigated a naturally derived lung surfactant, Infasurf, mixed with three polymeric NPs with varying hydrophobicities through the use of a Langmuir trough and atomic force microscopy to probe the intricacies at the air–water interface. In addition, a novel technique, constrained drop surfactometer (CDS), was used to gain insight on how NPs affect surfactant under physiological conditions. We found that the CDS can be used as a sensitive precautionary tool for identifying surfactant inhibition by NPs. Our data suggest that increasing surface hydrophobicity of NPs yields more retention in the surfactant monolayer and a higher degree of surfactant inhibition.

KEYWORDS: Nanoparticle, Lung surfactant, Hydrophobicity, Surface tension, Monolayer



INTRODUCTION

Interest in nanoscience and nanotechnology has grown immensely, particularly for its applications in nanomedicine and nanotoxicology.^{1,2} Much emphasis has been put on the pulmonary system as a portal of entry for nanoparticles (NPs) due to its administration ease and direct systemic access.^{3,4} When NPs are inhaled, the first biological barrier they interact with is the native pulmonary surfactant (PS) system.^{5,6} The PS has several physiological and biophysical functions that are essential for normal lung function and immune health.⁷ Lack or dysfunction of PS can cause pathological pulmonary conditions related to acute lung injury (ALI) or acute respiratory distress syndrome (ARDS),⁸ so it is crucial to preserve functional PS to maintain pulmonary health.

The PS is a complex mixture of mostly lipids (~90% by weight) and four surfactant proteins (SP-A, B, C, and D, ~10% by weight) that lines the entire alveolar surface as a thin film.⁷ A closer evaluation of the lipid portion of PS reveals that the majority of the lipids are phospholipids that contribute to its high surface activity (i.e., the ability to reduce alveolar surface tension to near-zero). SP-A and SP-D are hydrophilic proteins that assist in macrophage clearance and other innate immune responses.⁹ The other two proteins, SP-B and SP-C, are hydrophobic proteins embedded in the phospholipid matrix that work in coordination with phospholipids to achieve low surface tension during respiration cycles.¹⁰

The interactions of NPs and PS films are largely not understood, but it has been shown that the physicochemical characteristics of NPs are ultimately a determining factor in their interaction behavior.^{11–15} One defining characteristic that has been shown to be integral in a nanobio interaction is the hydrophobicity of NPs.^{15–19} Reports have shown that hydrophobic NPs induce PS inhibition much more readily and to a higher degree than hydrophilic NPs.^{15,16} In addition to surfactant inhibition, recent molecular dynamics simulations have predicted that hydrophobicity also governs the NP translocation behavior through PS monolayer.¹⁵ The translocation behavior ultimately determines if a particle can quickly reach the pulmonary epithelia or if it will be retained at the air–water interface of the lung for a prolonged period of time. However, experimental correlation between particle retention and surfactant inhibition due to hydrophobic NPs has not been established.

In this paper, we experimentally studied how three polymeric NPs with varying relative hydrophobicities affect, *in vitro*, biophysical properties of an animal-derived surfactant preparation, Infasurf. We first characterized the hydrophobicity of these

Special Issue: Sustainable Nanotechnology 2013

Received: February 16, 2014

Revised: April 24, 2014

Published: April 30, 2014

three NPs using the Rose Bengal partitioning method. Subsequently, we studied the translocation/retention behavior of these NPs at the Infasurf monolayer using the combination of a classical Langmuir–Blodgett trough and atomic force microscopy (AFM). Finally, we evaluated surfactant inhibition caused by these three NPs under physiologically relevant conditions using a newly developed experimental method called the constrained drop surfactometer (CDS). All of these experiments showed consistent results and indicated that increasing surface hydrophobicity of NPs provokes their retention at the surfactant monolayer and deteriorates surface activity of PS.

■ EXPERIMENTAL SECTION

Pulmonary Surfactant. Infasurf (calfactant) is a gift from ONY, Inc. (Amherst, NY). It is a modified natural surfactant prepared from lung lavage of newborn calves by centrifugation and organic solvent extraction. Infasurf contains all hydrophobic components of the bovine natural surfactant. Hydrophilic surfactant proteins (SP-A and SP-D), however, were removed during the extraction process. Infasurf was stored frozen in sterilized vials with an initial concentration of 35 mg of total phospholipids per milliliter. On the day of the experiment, it was diluted by a saline buffer of 0.9% NaCl, 1.5 mM CaCl₂, and 2.5 mM HEPES, adjusted to pH 7.0.

Nanoparticles. Poly(D,L-lactide-co-glycolide) 53/47 with an intrinsic viscosity of 0.2 dL/g (acid-terminated PLGA; abbreviated P02A) and 1.03 dL/g (ester-terminated PLGA; abbreviated P103E) were purchased from Purac (Gorinchem, The Netherlands). P02A and P103E nanoparticles were synthesized by a water-in-oil emulsion solvent evaporation technique and stabilized with PVA. Polystyrene (PST) nanoparticles were purchased from Thermo Scientific (3090A Nanosphere Size Standards, Fremont, CA). All NPs were characterized for their primary size, hydrodynamic size, surface charge, and surface hydrophobicity. The primary size of the NPs was determined by analyzing FESEM and TEM (Hitachi HT7700) images with the ImageJ software ($n = 20$). The hydrodynamic size and zeta potential of the NPs were determined at a dilute particle concentration of 0.01 mg/mL under the same buffering condition of the natural PS, i.e., 0.9% NaCl, 1.5 mM CaCl₂, and 2.5 mM HEPES, at pH 7.0. The hydrodynamic size was measured using a Brookhaven 90Plus/BI-MAS particle sizer (Holtville, NY, U.S.A.). Zeta potential was determined using a Brookhaven ZetaPlus zeta potential analyzer. The surface hydrophobicity was measured with the Rose Bengal partitioning method.

Rose Bengal Partitioning. Hydrophobicity of the NPs was studied using the Rose Bengal partitioning method as previously described.²⁰ A solution of Rose Bengal (RB) reagent (Sigma-Aldrich, St. Louis, MO) in a 0.1 M phosphate buffer (pH 7.4) was diluted to 20 $\mu\text{g/mL}$. Various concentrations of NPs were added to the solution to create a wide array of RB-NP suspensions. Each sample was incubated at 25 °C for 3 h. Suspensions were subsequently centrifuged at 16,000g for 1 h. The supernatant was collected and absorbance was read using a UV/vis spectrometer at 543 nm (Epoch, BioTek, Winooski, VT). Partitioning Quotient (PQ) was determined as the ratio of RB bound onto the particle surface to free RB in the liquid phase, i.e., $\text{PQ} = \text{RB}_{\text{bound}}/\text{RB}_{\text{free}}$. A plot of PQ versus surface area was made. The slope of the linear regression line can be used as an accurate representation of relative surface hydrophobicity, where increasing slope correlates with increasing surface hydrophobicity.²⁰

Langmuir–Blodgett Trough and AFM. Spread, compression, and Langmuir–Blodgett (LB) transfer of surfactant films were conducted with a LB trough (KSV Nima, Coventry, U.K.) at room temperature (20 ± 1 °C). Detailed experimental protocol can be found elsewhere.¹⁴ Briefly, all three NPs were diluted to 50 $\mu\text{g/mL}$ with a 5 mg/mL Infasurf suspension, i.e., 1% NP to surfactant by weight. This NP-PS suspension was spread atop a Milli-Q water subphase. The spread films were compressed at a rate of 40 cm^2/min , namely, 0.2% initial surface area per second. For AFM imaging, spread

films at the air–water interface were transferred to the surface of freshly cleaved mica using the LB technique. Transferred films were scanned by an Innova AFM (Bruker, Santa Barbara, CA) in air with the contact mode. Each sample was characterized at multiple locations with various scan areas to ensure the detection of representative structures.

Constrained Drop Surfactometer. *In vitro* simulations of surfactant activity and inhibition under physiologically relevant conditions were studied with a constrained drop surfactometer (CDS). The CDS is a droplet-based surface tensiometer, newly developed for *in vitro* assessing biophysical properties of lung surfactant.^{21,22} The CDS uses the air–water interface of a sessile drop (~ 3 mm), constrained on a carefully machined drop pedestal with a sharp knife-edge, to accommodate the adsorbed surfactant films.⁷ Hence, the CDS requires only a minute sample size of about 10 μL for studying lung surfactant. Also owing to system miniaturization, the CDS permits a precise control of physiological conditions using an environmental control chamber. To simulate breathing, the droplet can be compressed and expanded at a physiologically relevant rate using a motorized syringe. The surface tension and surface area are determined photographically from the shape of the droplet using axisymmetric drop shape analysis (ADSA).²³ Compared to the Wilhelmy plate method used in the classical Langmuir balance, ADSA measures surface tension accurately and remotely, thus minimizing potential sample contamination and facilitating undisturbed drop oscillation.

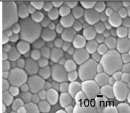
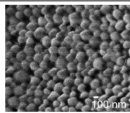
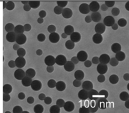
Specifically, Infasurf was diluted to a concentration of 1 mg/mL and mixed with NPs to a final NP concentration of 10 $\mu\text{g/mL}$, i.e., 1% NP to surfactant by weight. This NP concentration was selected corresponding to the lower end of NP concentrations tested in previous studies.^{11–16} The NPs were incubated with Infasurf at 37 °C for 1 h before cycling trials commenced. A droplet (~ 10 μL) of the NP–Infasurf mixture was dispensed onto the CDS drop pedestal. After drop formation, the surface tension was recorded and found to quickly decrease to an equilibrium value of approximately 22–25 mN/m. Once equilibrium was established, the droplet was compressed and expanded at a rate of 3 s per cycle with a compression ratio controlled to be less than 50% of the initial surface area to simulate normal tidal breathing.²⁴ At least five continuous compression–expansion cycles were studied for each droplet. It was found that the cycles became repeatable right after the first cycle, similar to surfactant behavior in a captive bubble surfactometer (CBS).^{25,26} Surface activity was quantified with several parameters: minimum surface tension (γ_{min}) at the end of compression, maximum surface tension (γ_{max}) at the end of expansion, and film compressibility, $\kappa = (1/A)(\partial A/\partial \gamma)$, during both the compression and expansion processes. Given the fact that κ varies during the compression and expansion processes, an averaged κ value was compared for each process. All simulations were conducted under well-controlled physiological conditions (37 °C and 100% RH).

Statistical Analysis. Statistical data were represented by the mean \pm SEM. The measurements were based on dynamic cycling data for Infasurf ($n = 9$), Infasurf + P02A ($n = 7$), Infasurf + P103E ($n = 7$), and Infasurf + PST ($n = 7$). One-way ANOVA was used for statistical calculations (OriginPro, Northampton, MA). Tukey and Bonferroni means comparison tests were used, and a probability value of $p < 0.05$ was considered statistically significant.

■ RESULTS AND DISCUSSION

Characterization of NPs. We first characterized the morphology and surface properties of the three NPs in a study, i.e., P02A, P103E, and PST. As shown in Table 1, all NPs are spherical in shape and have mean primary sizes of 231, 264, and 84 nm, respectively. The mean hydrodynamic sizes of these NPs in buffer were measured to be 260, 350, and 95 nm, respectively, thus indicating no significant particle aggregation. Surface charge measurement by ζ -potential showed that all NPs were negatively charged to a similar degree. Surface hydrophobicity was measured by comparing the adsorption of Rose

Table 1. Morphological and Surface Characterization of Nanoparticles

Particle	Acid-terminated PLGA (P02A)	Ester-terminated PLGA (P103E)	Polystyrene (PST)
Electron Microscopy			
Primary Size (nm)	231 ± 41	264 ± 55	84 ± 13
Hydrodynamic Size (nm)	260 ± 8	350 ± 7	95 ± 3
ζ-Potential (mV)	-17 ± 0.5	-15 ± 0.1	-27 ± 0.6
Hydrophobicity (10 ⁻⁹ mL/μm ²)	0.012 ± 0.002	0.025 ± 0.003	0.069 ± 0.009

Bengal, a hydrophobic dye, to the NPs. A plot of partitioning quotient (PQ) versus NP surface area per milliliter is constructed in Figure 1. The slope of this plot has been used

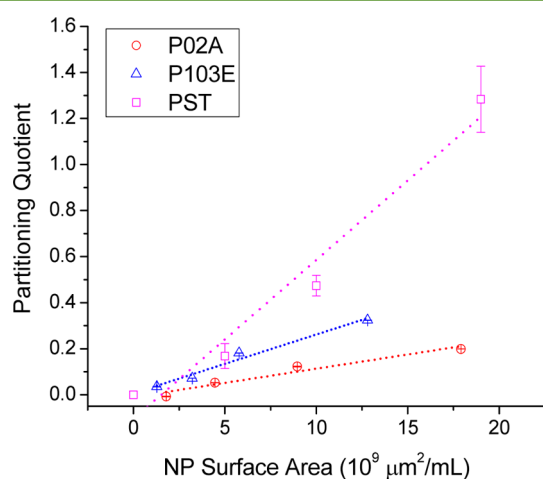


Figure 1. Hydrophobicity measurements via Rose Bengal partitioning. The three particles' linear relationships of partitioning quotient vs surface area are plotted. Linear regression lines are then calculated where the slopes are proportional to the relative hydrophobicity of the NPs. These data show that the particles' hydrophobicity increases in such a manner that P02A is the least hydrophobic, P103E has moderate hydrophobicity, and PST is the most hydrophobic.

recurrently as an accurate representation of surface hydrophobicity, where increasing slope is proportional to increasing hydrophobicity of NPs.^{16,20,27,28} PST (0.069×10^{-9} mL/μm²) yielded the highest slope, followed by P103E (0.025×10^{-9} mL/μm²), and P02A (0.012×10^{-9} mL/μm²) showed the lowest slope. These results indicate that relative to one another, PST is the most hydrophobic, followed by P103E, and P02A is the least hydrophobic of the three.

Particle Retention at the Surfactant Monolayer. We first studied NP-PS interaction and particle retention using the combination of LB trough and AFM. Compression isotherms were measured for pure Infasurf, Infasurf + P02A, Infasurf + P103E, and Infasurf + PST (Figure 2A). The exposure of all three NPs shifted the compression isotherm of Infasurf to the left. This shift indicates the compressibility (κ) of the film is increased when NPs are introduced, i.e., more area compression is necessary for the Infasurf + NP films to attain the same arbitrary surface pressure compared to pure Infasurf. Note that

the surface pressure (π) of a monolayer is inversely related to its surface tension (γ) by $\pi = \gamma_0 - \gamma$, in which γ_0 is the surface tension of pure water. Hence, the shift of the compression isotherm to the lower surface area region indicates that all three NPs inhibited the surface activity of Infasurf, i.e., decreased its ability to reduce surface tension upon film compression.

AFM topographical images of the surfactant film for pure Infasurf as well as Infasurf mixed with NPs at four characteristic surface pressures were taken to examine lateral film structures (Figure 2B). It is found that the addition of NPs inhibited phospholipid phase transitions, as revealed by reduced phospholipid domains at the surfactant monolayer. At a π of 50 mN/m, the Infasurf monolayer was transformed into a multilayered structure with uniformly distributed lipid protrusions closely attached to the interfacial surfactant monolayer. However, at 50 mN/m (which is also the collapse pressure of the Infasurf film exposed to NPs), addition of all NPs disturbed this normal conformational monolayer-to-multilayer transformation by forming nonuniform large protrusions comparable to the hydrodynamic size of the respective NPs.

A similar disturbance of surfactant monolayer has been found with other NPs.^{13–15,19} Phospholipid phase transitions are considered to be necessary for normal biophysical function of lung surfactant, at least under *in vitro* conditions.²⁹ Meanwhile, uniform monolayer-to-multilayer transformations have been proven to be a necessity for lung surfactant to reach physiologically relevant low surface tensions (or high surface pressures).^{30,31} Disturbance of phospholipid phase transition and monolayer-to-multilayer transformation by the addition of NPs appears to cause surfactant inhibition shown in Figure 2A.

More interestingly, AFM revealed that with increasing surface hydrophobicity the frequency of NP aggregates visualized at the surfactant monolayer also increased. While the least hydrophobic NPs, P02A, only appeared at the surface at 50 mN/m. The most hydrophobic NPs, PST, were found at much lower surface pressures (20 mN/m), indicating a strong correlation between surface hydrophobicity of NPs and their retention/translocation behavior at the surfactant monolayer. It should be noted that in addition to surface hydrophobicity, hydrodynamic sizes of these three NPs are also different. Many studies have shown that size and shape of NPs determine their translocation behavior across lipid monolayers/bilayers or even cell membranes,³² with larger particles encountering a higher energy barrier for translocation. However, the size of PST used in this study is smaller than the other two NPs. Hence, the higher retention rate of PST at the Infasurf monolayer can be only related to its higher hydrophobicity.

This finding is in good agreement with our recent molecular dynamics simulations in which we found that hydrophobicity is the determining factor for NP translocation/retention at the surfactant monolayer.¹⁵ Our molecular dynamics simulations further predicted that hydrophobic NPs can be encapsulated by a surfactant lipoprotein corona and trapped at the surfactant monolayer upon compression.¹⁵ These *in silico* results are also consistent with our current *in vitro* measurements (Figure 2B), which show that the height of large protrusions formed at the surfactant monolayer is comparable to the actual hydrodynamic size of the respective NPs.

Our present *in vitro* findings in the retention of hydrophobic PST NPs at the surfactant monolayer may be related to previous animal trials.^{33–35} Both *ex vivo* and *in vivo* experiments demonstrated that intratracheally instilled PST NPs, in a size

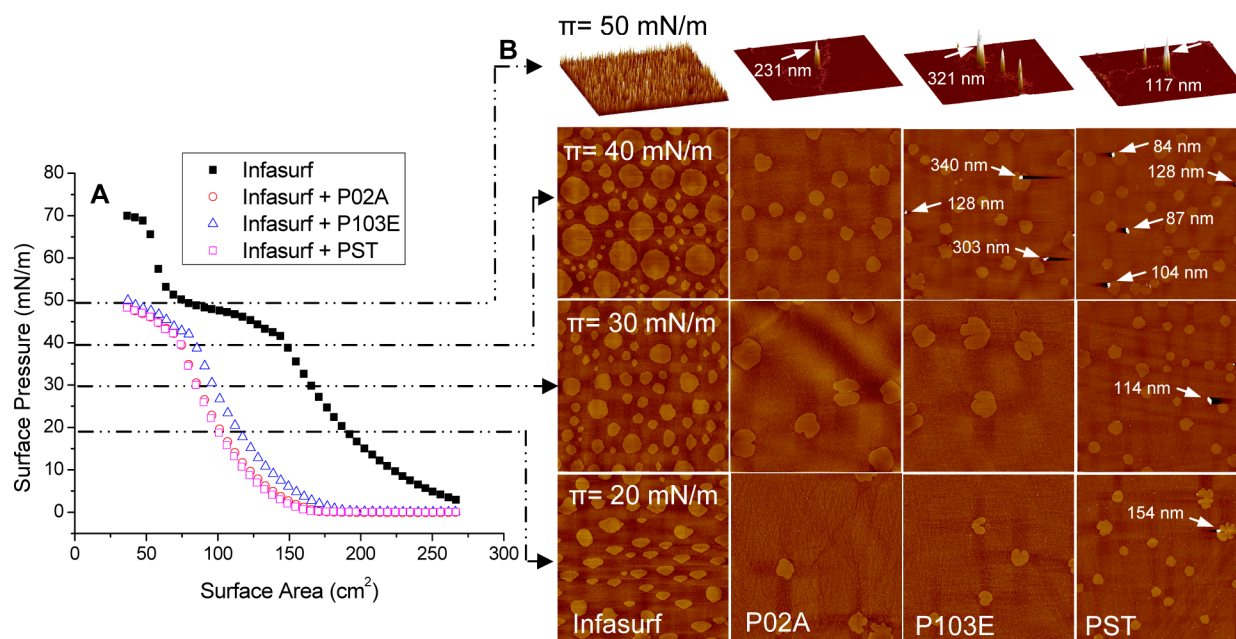


Figure 2. Comparison of NP retention at the Infasurf film. (A) Effect of 50 $\mu\text{g}/\text{mL}$ NPs (i.e., 1% w/w of surfactant phospholipids) on the compression isotherm of Infasurf. (B) Lateral film structures of pure Infasurf and Infasurf mixed with P02A, P103E, and PST at four characteristic surface pressures (20, 30, 40, and 50 mN/m). All monolayer images (20, 30, and 40 mN/m) are shown at a resolution of $50\ \mu\text{m} \times 50\ \mu\text{m}$ and have a z-range of 5 nm. The multilayer structures are all shown at a resolution of $20\ \mu\text{m} \times 20\ \mu\text{m}$, and their z-ranges are dependent on the size of the particle (Infasurf, 20 nm; Infasurf + P02A, 250 nm; Infasurf + P103E, 350 nm; and Infasurf + PST, 120 nm). These high pressure images are shown in 3D to capture the topographic contrast between the particles and multilayer structures. The presence of NPs, denoted by white arrows, increases with increasing hydrophobicity. After the monolayer-to-multilayer transition (at 50 mN/m), all three NPs are found at the surface and embedded in the large multilayer protrusions. In contrast, pure Infasurf shows uniform protrusions that line the entire film surface.

range comparable to what we studied here, showed very limited translocation from the lungs.^{33–35} Prolonged retention of NPs in the lungs can have a significant toxicological effect due to increased production of reactive oxygen species (ROS) and, in turn, increased inflammatory potential.

Physiologically Relevant Study of Surfactant Inhibition. Self-assembled monolayer at the air–water interface of a Langmuir trough is a commonly used *in vitro* model for studying lung surfactant. However, data obtained from such experiments have only limited physiological relevance due to commonly uncontrolled environmental conditions, relatively slow rate of film oscillation, and other design limitations.⁷ In order to conduct physiologically relevant *in vitro* simulations, we studied surfactant inhibition using the constrained drop surfactometer (CDS), in which a surfactant droplet is oscillated at a physiologically relevant rate and the environment is manipulated to mimic physiological conditions.

Figure 3 compares typical compression–expansion cycles of pure Infasurf and Infasurf mixed with P02A, P103E, and PST nanoparticles. It is observed that all three NPs significantly increased the hysteresis area of the compression–expansion loop. More importantly, the hysteresis area increased with increasing surface hydrophobicity of the NPs. Large hysteresis areas of dynamic cycling loops are a strong indication of film instability and surfactant inhibition.^{25,26} Therefore, our *in vitro* simulations with the CDS not only demonstrated a NP-induced surfactant inhibition, which is consistent with our Langmuir trough studies (Figure 2A), but also revealed a NP hydrophobicity-dependent inhibitory potency, which the Langmuir trough was not sensitive enough to uncover.

To completely understand the effects of the three NPs on dynamic surface activity of Infasurf, statistical analyses of the

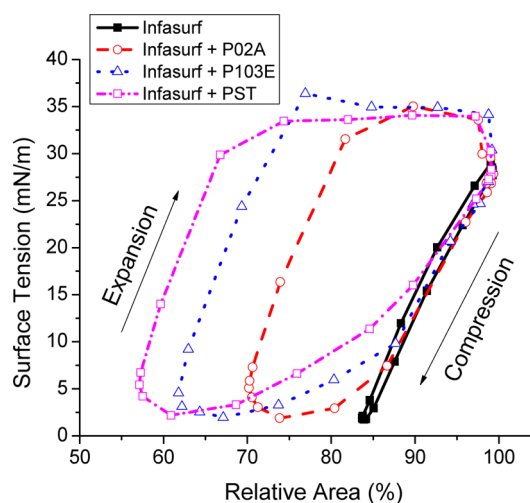


Figure 3. Comparison of compression–expansion cycles for pure Infasurf and Infasurf mixed with NPs. Cycling data for pure Infasurf and Infasurf mixed with P02A, P103E, and PST are represented by overlying surface tension vs surface area plots. Infasurf was diluted to a concentration of 1 mg/mL and mixed with NPs to 10 $\mu\text{g}/\text{mL}$, i.e., 1% NP:surfactant (w/w). Dynamic cycling was conducted with the CDS under physiological temperature (37 $^{\circ}\text{C}$) and cycling speed (3 s/cycle). It is observed that the hysteresis area of the compression–expansion loop increases significantly with increasing NP hydrophobicity.

data were performed (Figures 4). Figure 4A shows the comparison of minimum surface tension (γ_{min}) at the end of compression and maximum surface tension (γ_{max}) at the end of expansion. It is observed that the γ_{min} shows a statistically

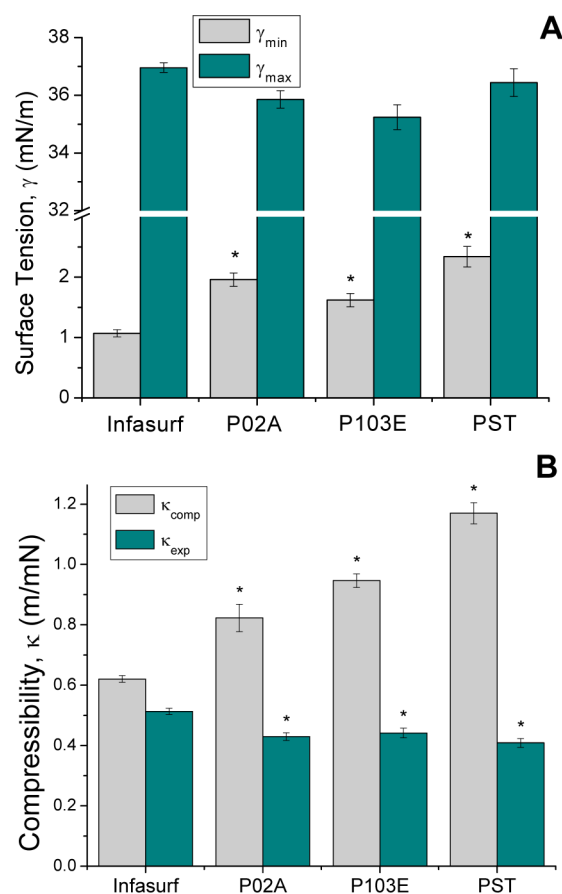


Figure 4. Statistical analysis of the effect of NPs on surface activity of Infasurf. (A) Minimum surface tension (γ_{\min}) at the end of compression and maximum surface tension (γ_{\max}) at the end of expansion for Infasurf and mixed Infasurf + NP suspensions. (B) Film compressibility during compression (κ_{comp}) and expansion (κ_{exp}) processes for Infasurf and mixed Infasurf + NP suspensions. Each trial was conducted with the CDS at 37 °C and cycled at a physiologically relevant rate (3 s/cycle). * $p < 0.05$ for comparison to pure Infasurf.

significant increase due to exposure to all three NPs, although a very low particle concentration (i.e., 10 $\mu\text{g}/\text{mL}$) was used. However, with all NPs, Infasurf was still able to achieve a γ_{\min} below 3 mN/m. Hence, the variations in γ_{\min} due to exposure to these low-concentration NPs can be considered physiologically immaterial. Similarly, the γ_{\max} shows no statistically significant changes with the addition of NPs. The lack of a physiologically significant alteration of surface tension is consistent with Beck-Broichsitter et al., who demonstrated that γ_{\min} only showed a significant increase when exposed to PST NP concentrations greater than 1 mg/mL, i.e., NP weight greater than 50% of surfactant weight in their experiments.¹⁷

Figure 4B shows the comparison of film compressibility (κ) during both compression and expansion processes. Addition of all three NPs, at a very low concentration of 10 $\mu\text{g}/\text{mL}$, significantly increased the κ of Infasurf during compression (κ_{comp}) and decreased the κ during expansion (κ_{exp}). The increase in κ_{comp} is clearly proportional to hydrophobicity of the NPs. It should be noted that differences in κ_{comp} were statistically significant between all four groups, indicating that surface hydrophobicity of NPs plays a significant role in affecting surfactant inhibition.

It is known that κ is a much more sensitive parameter than γ_{\min} to evaluate surface activity and surfactant inhibition.^{22,36}

Compressibility of a monolayer can be loosely related to its “hardness”. A low κ indicates a strong film, while a high κ indicates a soft film. A good lung surfactant film should have a soft-yet-strong attribute.⁷ Upon film compression during exhalation, the surfactant film should have a low κ , thus decreasing alveolar γ (equivalent to increasing π) to near-zero with less than 20% area compression.^{22,36} Upon film expansion during inhalation, the surfactant film should have a high κ , thus only increasing γ to a limited value. Although still unclear in detailed mechanisms, lung surfactant appears to achieve this soft-yet-strong attribute by selective compositional and/or conformational variations during the compression–expansion cycles.^{30,31,37} It appears that addition of NPs inhibits surface activity of lung surfactant by increasing κ_{comp} and decreasing κ_{exp} (Figure 4B), thus increasing the hysteresis area of the compression–expansion loop (Figure 3).

Previous studies suggested that NPs inhibit lung surfactant by adsorbing surfactant proteins (such as SP-B and SP-C), i.e., through the formation of native surfactant lipoprotein corona.^{14–16,38} After binding to solid particles, surfactant proteins can be denatured and/or depleted from the surfactant system, thereby causing surfactant inhibition. More hydrophobic NPs have a higher retention rate at the surfactant monolayer (Figure 2) and hence a higher chance of adsorbing surfactant proteins. Consequently, more hydrophobic NPs appear to have a higher inhibitory potential to lung surfactant (Figures 3 and 4).

In addition to surfactant inhibition, prolonged retention of hydrophobic NPs at the surfactant monolayer may have a significant toxicological effect. A major contributor in NP-associated pulmonary nanotoxicology is the increase in reactive oxygen species (ROS) and, in turn, inflammation.^{39,40} It has been reported that more hydrophobic NPs are associated with a larger magnitude of ROS production and inflammation.³⁹ Dailey et al. demonstrated that PST NPs showed considerably higher nanotoxicological effects than PLGA at the same size, surface area, and concentration.⁴⁰ Very recently, Dailey and co-workers established the direct correlation between NP hydrophobicity and pulmonary toxicity.⁴¹ They found that intratracheal administration of more hydrophobic NPs (with PST NPs being the most hydrophobic) to mice induced acute respiratory toxicity revealed by neutrophil infiltration, elevation of pro-inflammatory cytokines, and adverse histopathology findings, while less hydrophobic NPs caused little or no inflammatory response or tissue damage.⁴¹ Although the underlying relationship between the pulmonary toxicity of hydrophobic NPs and their inhibitory potential on lung surfactant is yet to be developed, our current *in vitro* data clearly support such correlations.

In conclusion, we found that hydrophobicity of NPs plays an important role in affecting their retention at the surfactant monolayer and their inhibitory potential on surface activity of pulmonary surfactant. Increasing hydrophobicity ultimately increases NP retention and exacerbates surfactant inhibition. We also showed that the constrained drop surfactometer (CDS) developed in our laboratory can be used as a sensitive precautionary tool for probing surfactant inhibition by nanoparticles.

■ AUTHOR INFORMATION

Corresponding Author

*E-mail: yzuo@hawaii.edu. Tel: 808-956-9650. Fax: 808-956-2373.

Notes

The authors declare no competing financial interest.

ACKNOWLEDGMENTS

We thank Dr. Walter Klein at ONY, Inc. for donation of Infasurf samples. This work was supported by NSF Grant No. CBET-1236596 (Y.Y.Z.).

REFERENCES

- (1) Oberdorster, G.; Oberdorster, E.; Oberdorster, J. Nanotoxicology: An emerging discipline evolving from studies of ultrafine particles. *Environ. Health Perspect.* **2005**, *113* (7), 823–39.
- (2) Kim, B. Y.; Rutka, J. T.; Chan, W. C. Nanomedicine. *N. Engl. J. Med.* **2010**, *363* (25), 2434–2443.
- (3) Yang, W.; Peters, J. I.; Williams, R. O., 3rd Inhaled nanoparticles—A current review. *Int. J. Pharm.* **2008**, *356* (1–2), 239–247.
- (4) Muhlfield, C.; Rothen-Rutishauser, B.; Blank, F.; Vanhecke, D.; Ochs, M.; Gehr, P. Interactions of nanoparticles with pulmonary structures and cellular responses. *Am. J. Physiol. Lung Cell Mol. Physiol.* **2008**, *294* (5), L817–829.
- (5) Schleh, C.; Hohlfeld, J. M. Interaction of nanoparticles with the pulmonary surfactant system. *Inhal. Toxicol.* **2009**, *21*, 97–103.
- (6) Monopoli, M. P.; Aberg, C.; Salvati, A.; Dawson, K. A. Biomolecular coronas provide the biological identity of nanosized materials. *Nat. Nanotechnol.* **2012**, *7* (12), 779–86.
- (7) Zuo, Y. Y.; Veldhuizen, R. A.; Neumann, A. W.; Petersen, N. O.; Possmayer, F. Current perspectives in pulmonary surfactant—Inhibition, enhancement and evaluation. *Biochim. Biophys. Acta* **2008**, *1778* (10), 1947–1977.
- (8) Lewis, J. F.; Veldhuizen, R. The role of exogenous surfactant in the treatment of acute lung injury. *Annu. Rev. Physiol.* **2003**, *65*, 613–642.
- (9) Ruge, C. A.; Schaefer, U. F.; Herrmann, J.; Kirch, J.; Canadas, O.; Echaide, M.; Perez-Gil, J.; Casals, C.; Muller, R.; Lehr, C. M. The interplay of lung surfactant proteins and lipids assimilates the macrophage clearance of nanoparticles. *PLoS One* **2012**, *7* (7), e40775.
- (10) Perez-Gil, J. Structure of pulmonary surfactant membranes and films: The role of proteins and lipid-protein interactions. *Biochim. Biophys. Acta* **2008**, *1778* (7–8), 1676–1695.
- (11) Bakshi, M. S.; Zhao, L.; Smith, R.; Possmayer, F.; Petersen, N. O. Metal nanoparticle pollutants interfere with pulmonary surfactant function in vitro. *Biophys. J.* **2008**, *94* (3), 855–868.
- (12) Schleh, C.; Muhlfield, C.; Pulskamp, K.; Schmiedl, A.; Nassimi, M.; Lauenstein, H. D.; Braun, A.; Krug, N.; Erpenbeck, V. J.; Hohlfeld, J. M. The effect of titanium dioxide nanoparticles on pulmonary surfactant function and ultrastructure. *Respir. Res.* **2009**, *10*, 90.
- (13) Sachan, A. K.; Harishchandra, R. K.; Bantz, C.; Maskos, M.; Reichelt, R.; Galla, H. J. High-resolution investigation of nanoparticle interaction with a model pulmonary surfactant monolayer. *ACS Nano* **2012**, *6* (2), 1677–1687.
- (14) Fan, Q.; Wang, Y. E.; Zhao, X.; Loo, J. S.; Zuo, Y. Y. Adverse biophysical effects of hydroxyapatite nanoparticles on natural pulmonary surfactant. *ACS Nano* **2011**, *5* (8), 6410–6416.
- (15) Hu, G.; Jiao, B.; Shi, X.; Valle, R. P.; Fan, Q.; Zuo, Y. Y. Physicochemical properties of nanoparticles regulate translocation across pulmonary surfactant monolayer and formation of lipoprotein corona. *ACS Nano* **2013**, *7* (12), 10525–33.
- (16) Beck-Broichsitter, M.; Ruppert, C.; Schmehl, T.; Guenther, A.; Betz, T.; Bakowsky, U.; Seeger, W.; Kissel, T.; Gessler, T. Biophysical investigation of pulmonary surfactant surface properties upon contact with polymeric nanoparticles in vitro. *Nanomedicine* **2011**, *7* (3), 341–350.
- (17) Beck-Broichsitter, M.; Ruppert, C.; Schmehl, T.; Gunther, A.; Seeger, W. Biophysical inhibition of synthetic vs. naturally-derived pulmonary surfactant preparations by polymeric nanoparticles. *Biochim. Biophys. Acta* **2014**, *1838* (1), 474–481.
- (18) Dominguez-Medina, S.; Blankenburg, J.; Olson, J.; Landes, C. F.; Link, S. Adsorption of a protein monolayer via hydrophobic interactions prevents nanoparticle aggregation under harsh environmental conditions. *ACS Sustainable Chem. Eng.* **2013**, *1* (7), 833–842.
- (19) Tatur, S.; Badia, A. Influence of hydrophobic alkylated gold nanoparticles on the phase behavior of monolayers of DPPC and clinical lung surfactant. *Langmuir* **2012**, *28* (1), 628–639.
- (20) Muller, R. H.; Ruhl, D.; Luck, M.; Paulke, B. R. Influence of fluorescent labelling of polystyrene particles on phagocytic uptake, surface hydrophobicity, and plasma protein adsorption. *Pharm. Res.* **1997**, *14* (1), 18–24.
- (21) Yu, L. M. Y.; Lu, J. J.; Chan, Y. W.; Ng, A.; Zhang, L.; Hoorfar, M.; Policova, Z.; Grundke, K.; Neumann, A. W. Constrained sessile drop as a new configuration to measure low surface tension in lung surfactant systems. *J. Appl. Physiol.* **2004**, *97* (2), 704–715.
- (22) Zuo, Y. Y.; Alolabi, H.; Shafiei, A.; Kang, N.; Policova, Z.; Cox, P. N.; Acosta, E.; Hair, M. L.; Neumann, A. W. Chitosan enhances the in vitro surface activity of dilute lung surfactant preparations and resists albumin-induced inactivation. *Pediatr. Res.* **2006**, *60* (2), 125–130.
- (23) Zuo, Y. Y.; Do, C.; Neumann, A. W. Automatic measurement of surface tension from noisy images using a component labeling method. *Colloids Surf., A* **2007**, *299* (1–3), 109–116.
- (24) Bachofen, H.; Schurch, S.; Urbinelli, M.; Weibel, E. R. Relations among alveolar surface tension, surface area, volume, and recoil pressure. *J. Appl. Physiol.* **1987**, *62* (5), 1878–1887.
- (25) Schurch, S.; Bachofen, H.; Goerke, J.; Green, F. Surface properties of rat pulmonary surfactant studied with the captive bubble method: Adsorption, hysteresis, stability. *Biochim. Biophys. Acta* **1992**, *1103* (1), 127–136.
- (26) Schurch, S.; Green, F. H.; Bachofen, H. Formation and structure of surface films: Captive bubble surfactometry. *Biochim. Biophys. Acta* **1998**, *1408* (2–3), 180–202.
- (27) des Rieux, A.; Ragnarsson, E. G.; Gullberg, E.; Preat, V.; Schneider, Y. J.; Artursson, P. Transport of nanoparticles across an in vitro model of the human intestinal follicle associated epithelium. *Eur. J. Pharm. Sci.* **2005**, *25* (4–5), 455–465.
- (28) Xiao, Y.; Wiesner, M. R. Characterization of surface hydrophobicity of engineered nanoparticles. *J. Hazard. Mater.* **2012**, *215–216*, 146–151.
- (29) Casals, C.; Canadas, O. Role of lipid ordered/disordered phase coexistence in pulmonary surfactant function. *Biochim. Biophys. Acta* **2012**, *1818* (11), 2550–2562.
- (30) Zhang, H.; Fan, Q.; Wang, Y. E.; Neal, C. R.; Zuo, Y. Y. Comparative study of clinical pulmonary surfactants using atomic force microscopy. *Biochim. Biophys. Acta* **2011**, *1808*, 1832–1842.
- (31) Zhang, H.; Wang, Y. E.; Fan, Q.; Zuo, Y. Y. On the low surface tension of lung surfactant. *Langmuir* **2011**, *27* (13), 8351–8358.
- (32) Nel, A. E.; Madler, L.; Velegol, D.; Xia, T.; Hoek, E. M. V.; Somasundaran, P.; Klaessig, F.; Castranova, V.; Thompson, M. Understanding biophysicochemical interactions at the nano-bio interface. *Nat. Mater.* **2009**, *8* (7), 543–557.
- (33) Nemmar, A.; Hamoir, J.; Nemery, B.; Gustin, P. Evaluation of particle translocation across the alveolo-capillary barrier in isolated perfused rabbit lung model. *Toxicology* **2005**, *208* (1), 105–113.
- (34) Chen, J.; Tan, M.; Nemmar, A.; Song, W.; Dong, M.; Zhang, G.; Li, Y. Quantification of extrapulmonary translocation of intratracheal-instilled particles in vivo in rats: Effect of lipopolysaccharide. *Toxicol.* **2006**, *222* (3), 195–201.
- (35) Mills, N. L.; Amin, N.; Robinson, S. D.; Anand, A.; Davies, J.; Patel, D.; de la Fuente, J. M.; Cassee, F. R.; Boon, N. A.; Macnee, W.; Millar, A. M.; Donaldson, K.; Newby, D. E. Do inhaled carbon nanoparticles translocate directly into the circulation in humans? *Am. J. Respir. Crit. Care Med.* **2006**, *173* (4), 426–431.
- (36) Schurch, S.; Schurch, D.; Curstedt, T.; Robertson, B. Surface activity of lipid extract surfactant in relation to film area compression and collapse. *J. Appl. Physiol.* **1994**, *77* (2), 974–986.
- (37) Keating, E.; Zuo, Y. Y.; Tadayyon, S. M.; Petersen, N. O.; Possmayer, F.; Veldhuizen, R. A. A modified squeeze-out mechanism for generating high surface pressures with pulmonary surfactant. *Biochim. Biophys. Acta* **2012**, *1818* (5), 1225–1234.

(38) Sund, J.; Alenius, H.; Vippola, M.; Savolainen, K.; Puustinen, A. Proteomic characterization of engineered nanomaterial-protein interactions in relation to surface reactivity. *ACS Nano* **2011**, *5* (6), 4300–4309.

(39) Gasser, M.; Wick, P.; Clift, M. J.; Blank, F.; Diener, L.; Yan, B.; Gehr, P.; Krug, H. F.; Rothen-Rutishauser, B. Pulmonary surfactant coating of multi-walled carbon nanotubes (MWCNTs) influences their oxidative and pro-inflammatory potential in vitro. *Part. Fibre Toxicol.* **2012**, *9*, 17.

(40) Dailey, L. A.; Jekel, N.; Fink, L.; Gessler, T.; Schmehl, T.; Wittmar, M.; Kissel, T.; Seeger, W. Investigation of the proinflammatory potential of biodegradable nanoparticle drug delivery systems in the lung. *Toxicol. Appl. Pharmacol.* **2006**, *215* (1), 100–108.

(41) Jones, M. C.; Jones, S. A.; Riffo-Vasquez, Y.; Spina, D.; Hoffman, E.; Morgan, A.; Patel, A.; Page, C.; Forbes, B.; Dailey, L. A. Quantitative assessment of nanoparticle surface hydrophobicity and its influence on pulmonary biocompatibility. *J. Controlled Release* **2014**, *183C*, 94–104.